Journal of Glaciology, Vol. 44, No. 148, 1998

Glaciohydraulic supercooling: a freeze-on mechanism to create stratified, debris-rich basal ice: I. Field evidence

DANIEL E. LAWSON,[1] JEFFREY C. STRASSER,[2,3] EDWARD B. EVENSON,[3] RICHARD B. ALLEY,[4]
GRAHAME J. LARSON,[5] STEVEN A. ARCONE[6]

[1]*U.S. Army Cold Regions Research and Engineering Laboratory, Anchorage, Alaska 99505, U.S.A.*
[2]*Department of Geology, Augustana College, Rock Island, Illinois 61201, U.S.A.*
[3]*Department of Earth and Environmental Sciences, Lehigh University, Bethlehem, Pennsylvania 18015, U.S.A.*
[4]*Earth System Science Center and Department of Geosciences, The Pennsylvania State University, University Park, Pennsylvania 16802, U.S.A.*
[5]*Department of Geological Sciences, Michigan State University, East Lansing, Michigan 48824, U.S.A.*
[6]*U.S. Army Cold Regions Research and Engineering Laboratory, Hanover, New Hampshire 03755, U.S.A.*

ABSTRACT. Debris-laden ice accretes to the base of Matanuska Glacier, Alaska, U.S.A., from water that supercools while flowing in a distributed drainage system up the adverse slope of an overdeepening. Frazil ice grows in the water column and forms aggregates, while other ice grows on the glacier sole or on substrate materials. Sediment is trapped by this growing ice, forming stratified debris-laden basal ice. Growth rates of $>0.1\ m\ a^{-1}$ of debris-rich basal ice are possible. The large sediment fluxes that this mechanism allows may have implications for interpretation of the widespread deposits from ice that flowed through other overdeepenings, including Heinrich events and the till sheets south of the Laurentian Great Lakes.

INTRODUCTION

Glaciers and ice sheets can entrain and transport significant amounts of basal sediment (Kamb and LaChapelle, 1964; Boulton, 1970; Gow and others, 1979; Herron and Langway, 1979; Lawson, 1979b; Echelmeyer and Zhongxiang, 1987; Sugden and others, 1987a, b; Sharp and others, 1994; Hubbard and Sharp, 1995). Sediment transport in basal ice is linked closely to the mechanisms by which glaciers move, the characteristics of the englacial and subglacial drainage systems, and the interactions between ice flow and glaciohydraulic processes (Lawson, 1993). Many mechanisms have been proposed for the origin of debris-laden basal ice (e.g. Kamb and LaChapelle, 1964; Weertman, 1964; Boulton, 1972; Gow and others, 1979; Alley, 1991; Iverson and Semmens, 1995; Alley and others, 1997). These theories fail, however, to account adequately for the full suite of physical and isotopic attributes of the basal zone of Matanuska Glacier, Alaska, U.S.A. (Lawson and Kulla, 1978; Lawson, 1979a, b, 1988).

In this paper, we present field observations and analytical evidence from Matanuska Glacier that lead us to propose "glaciohydraulic supercooling" as the primary mechanism creating the debris-laden stratified facies of the glacier's basal zone. Our hypothesis is that ice accretes to the glacier's sole from supercooled water flowing in a distributed subglacial drainage system and that significant quantities of sediment are entrained during the ice growth and accretion process.

We show that ice grows in supercooled water emerging from subglacially fed vents at the glacier's terminus during summer, when air temperatures are well above 0°C, and demonstrate that sediment is entrapped during ice growth, producing accretion features composed of laminated, debris-rich ice that is very similar to the stratified basal ice of Matanuska Glacier. We expect that this mechanism is active and produces sediment-rich zones and significant debris fluxes beneath other glaciers with appropriate hydrological conditions. Glaciohydraulic supercooling may therefore have significant implications for interpretation of the origin of glacial sediments and their former environments of deposition.

FIELD SITE

Matanuska Glacier is a large valley glacier that flows north from ice fields in the Chugach Mountains of south-central Alaska (Fig. 1). The glacier is approximately 45 km long, ranges in width from approximately 3 km near the equilibrium line to about 5 km in the terminal lobe, and ranges in elevation from about 3500 m at its highest source on Mount Marcus Baker to about 500 m at the terminus. The terminus remained in a relatively stable position for most of the last 200 years or more (Williams and Ferrians, 1961), but has thinned and retreated about $10–30\ m\ a^{-1}$ during the past decade (D. E. Lawson, unpublished data).

We have recently focused our investigations on the western area of the terminus, where 4–20 m thick sections of the basal zone are commonly exposed (Fig. 2). In a part of this area, the glacier flows into a small basin or overdeepening (Fig. 3), forming a topographic low in the ice surface and a steep, heavily crevassed ice face at its up-glacier edge. Along this section of the margin, pressurized subglacial water discharges from numerous vents, commonly numbering >60–70 during the height of the melt season. During peak discharge, 0.5–1 m high fountains form in a

https://doi.org/10.3189/S0022143000002069 Published online by Cambridge University Press

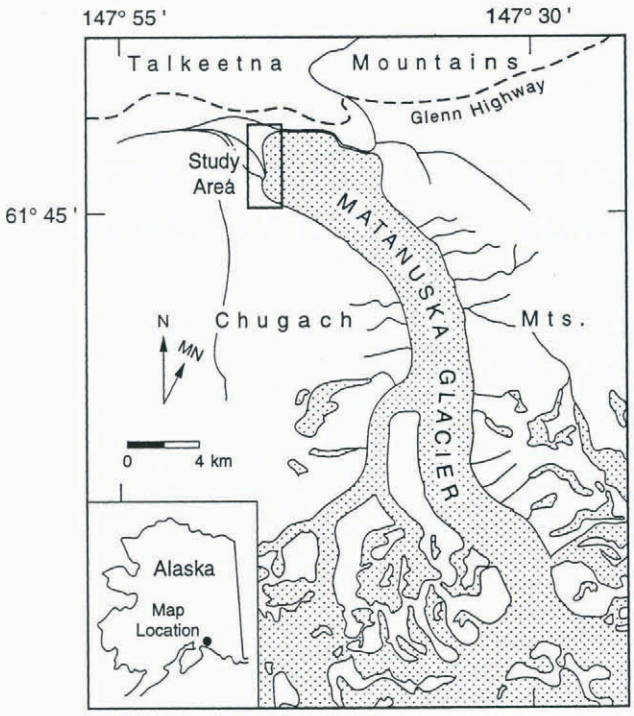

Fig. 1. Study area at Matanuska Glacier, Chugach Mountains, south-central Alaska.

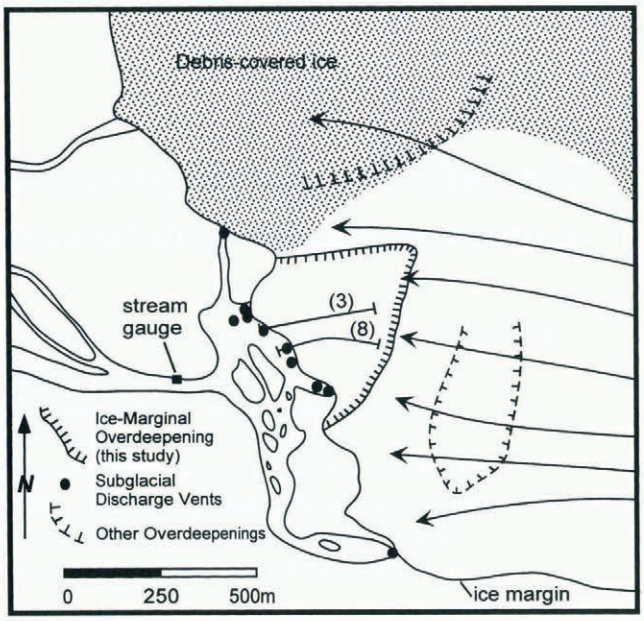

Fig. 3. General locations of subglacially fed vents and overdeepenings in the western terminus study area. Solid lines locate two GPR transects across the ice-marginal overdeepening (Fig. 9). Each solid dot locates an area of several or more square meters in which multiple vents discharge from the down-glacier edge of the ice-marginal overdeepening investigated in this study.

stream which runs along the glacier margin. Instantaneous discharge from individual vents ranges from about 0.03 $m^3 s^{-1}$ in smaller vents to 0.7 $m^3 s^{-1}$ in larger ones (J. Denner, U.S. Geological Survey, unpublished data, 1997).

A gauging station located approximately 200 m downstream of the terminus measures the combined discharge from all vents along the western margin (Fig. 3). Winter discharge is $\leq 1\ m^3 s^{-1}$ based on sparse measurements. It contains no suspended sediment and is presumably derived from groundwater, basal melting and drainage of water stored in the glacier. Discharge increases dramatically in the summer, with daily maxima of about 80 $m^3 s^{-1}$ during peak melt periods. Suspended-sediment concentrations range between 0.3 and 5.0 $g l^{-1}$, varying both daily and seasonally.

Fig. 2. Thick exposure of basal (dark, debris-rich) and englacial (white, debris-free) ice zones.

https://doi.org/10.3189/S0022143000002069 Published online by Cambridge University Press

ICE GROWTH IN SUBGLACIAL DISCHARGES

Water emerging from beneath Matanuska Glacier in summer is supercooled. Several lines of evidence indicate this condition. Frazil ice in this subglacial water is common as millimeter-sized particles, centimeter-sized plates, and flocs or aggregates of these particles and plates (Fig. 4a and b). Such highly visible particles and aggregates are inferred to originate from micrometer-sized crystals produced by heterogeneous nucleation in supercooled water (e.g. Michel, 1978; Ashton, 1986; Daly, 1994). In addition, the shape and dimensions of the observed frazil indicate growth since formation, and thus that they formed up-glacier in the subglacial drainage system, not simply at the point of discharge.

Dendritic and other platy crystals (disks, blades) grow on glacier and frazil ice, as well as on sediment that is in and around the conduits and vents (Fig. 4c), forming rims around them (Fig. 4a). Frazil ice also accumulates in cavities and other irregularities in the surfaces of vents and conduits. Ice grows between the frazil particles and dendritic crystals, eventually filling the pore spaces and creating a solid, anchored mass. Similarly, ice accumulates and grows in conduits located up-glacier of the terminus, as observed in conduits unroofed by ablation (e.g. Fig. 5).

Ice clusters or rosettes of smaller crystals that grow overnight on ropes and equipment suspended in vents and conduits are evidence of rapid formation (Fig. 6). Individual crystals can grow at rates of up to 30 mm d^{-1} (along their longest dimension). In just a few days of high discharge, ice on the walls of vents can grow fast enough to encompass equipment.

Anchor ice in vents grows terraces around upwellings and in supercooled water flowing away from vent centers (Fig. 7). Multi-tiered terraces can develop during extended periods of increasing discharge, while terraces from adjacent vents may coalesce to produce platforms that extend 20–30 m beyond the active glacier margin. Coalesced terraces can survive for years if they are buried deeply by sediment discharged from the vents.

The heights of terraces can exceed several meters, but are limited by water levels which fluctuate diurnally and seasonally in response to local weather conditions. Terraces exposed during warm weather ablate rapidly. Periodic ablation can concentrate sediment, forming debris-rich layers upon which additional ice grows. Repetition of this process can create a lamination of multiple subparallel layers with contrasting crystal sizes and debris contents.

Despite ablation during diurnal low-water stages and warm weather, we have observed ice terraces to grow rapidly over days. A net 70 mm of upward growth during 13 days of high discharge were recorded by spikes embedded in the surface of one terrace. At another location, the net vertical growth of a terrace was 1.5 m in 2 months. At both places, ice grew as intersecting crystalline plates, each plate exceeding 40 mm in length. Thin sections of this ice show a preferential growth along the crystallographic a axes into the supercooled water (Strasser and others, 1994).

The aggregates of platy crystals formed in up-glacier conduits and ice-marginal vents are initially highly permeable, and their open framework permits water to seep through the many interconnected pores (Fig. 8a). Fine-grained sediment in suspension can settle into voids as the water velocity is reduced within the ice mass. Subsequent epitaxial ice growth between the platy crystals traps the sediment between the grains and commonly produces debris-rich masses (Fig. 8b) with about 20–65% sediment by weight (about 10–40% by volume), based on 20 bulk samples. Such sediment typically consists of coarse silt and fine sand, but may also include gravel deposited from bedload during periods of higher discharge.

Frazil ice in transport, and the dendritic ice that grows in conduits, cavities and vents of Matanuska Glacier, show that water is supercooled in the subglacial drainage system. More importantly, the frazil flocs and aggregates that we see moving through the subglacial conduits provide further evidence that supercooled conditions developed some unknown distance up-glacier, not just at the point of discharge along the margin.

The magnitude of up-glacier subglacial supercooling is not known. In other environments, frazil forms in turbulently flowing water that is supercooled up to 0.01–0.02°C (Michel, 1978; Ashton, 1983; Osterkamp and Gosink, 1983; Daly, 1994; Forest, 1994). We have measured water temperatures 2 m down in the centers of vents at the ice margin, using individually calibrated thermistors ($\pm$0.015°C; resolution $\pm$0.003°C) and a Seabird Model 19 conductivity–temperature–depth (CTD) unit with U.S. National Bureau of Standards calibrated thermistors (referenced accuracy $\pm$0.003°C, resolution of $\pm$0.001°C). Temperatures ranged from −0.002° to −0.017°C.

NECESSARY CONDITIONS FOR SUPERCOOLING AND ICE GROWTH

Supercooling and ice accretion can be adequately explained by existing theory (Röthlisberger, 1972; Hooke, 1989; Alley and others, 1998). Water flowing up a sufficiently steep adverse slope of an overdeepening will not be warmed by viscous dissipation as rapidly as its pressure-melting temperature rises. Supercooling will lead to ice growth that tends to plug low-pressure channels and divert water flow. Water that remains along the glacier bed will be forced into a high-pressure, distributed system (Hooke, 1991; Hooke and Pohjola, 1994). Flow in this system can cause supercooling and ice growth across much of the glacier bed (Alley and others, 1998). Supercooling is possible for an adverse bed slope >1.2–1.7 times the magnitude of the surface slope, depending on the air-saturation state of the water (Röthlisberger, 1972; Hooke, 1991).

Ground-penetrating-radar (GPR) profiles from over 40 transects forming a grid across the terminus region provide data on the geometry of the ice-marginal overdeepening, and insights into its hydrology. The profiles were recorded with a 100 MHz short-pulse radar system along and perpendicular to the ice-flow direction during the early spring of 1991 before the onset of seasonal melting. The recorded data were horizontally filtered (before elevation corrections) to alleviate surface multiples, deconvolved to reduce wavelet resonance, and migrated using a Kirchhoff one-layer scheme to position the interfaces correctly and collapse diffractions (Arcone and others, 1995).

As reported previously (Lawson and others, 1991; Arcone and others, 1995), the radar profiles delineate the clean englacial and dirty basal ice zones (Lawson, 1979b), and give some indication of a transition from basal ice to subglacial sediment. Two zones occur in the englacial ice: an upper seasonally frozen zone with little liquid water, and a lower wet zone in which liquid water is apparently

https://doi.org/10.3189/S0022143000002069 Published online by Cambridge University Press

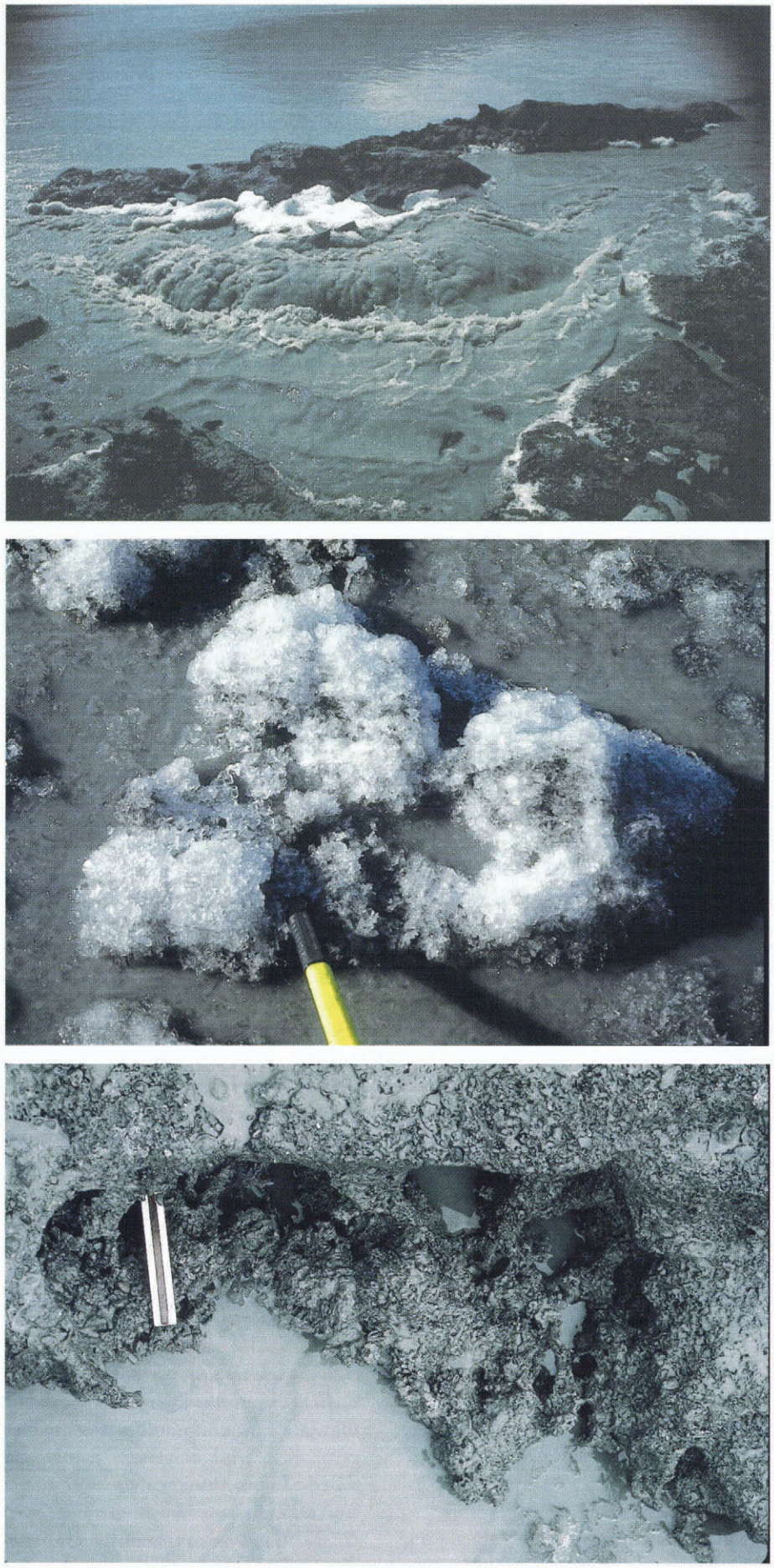

Fig. 4. Examples of vents and anchor and frazil ice in and around vents. (a) Three meter wide vent with raised (~300 mm) surface of upwelling water. White area is platy anchor ice exposed by the diurnal reduction in discharge; sediment which was discharged from the upwelling lies on other anchor ice surrounding the vent. (b) Aggregate or floc of frazil ice (~250 mm across) that was captured in a vent after emergence from a subglacial conduit. Tip of ice ax for scale. (c) Debris-laden anchor ice growing into a subglacial conduit exposed at low discharge. Note the upwelling vent water and the clean frazil flocs floating in it.

https://doi.org/10.3189/S0022143000002069 Published online by Cambridge University Press

Fig. 5. Conduit exposed by ablation of englacial ice. Sediment-laden, platy crystalline aggregate lines the conduit, which was located about 200 m up-glacier of the terminus. Sediment was filtered by the ice mass from that in water flowing through the mass.

present (Fig. 9). The basal-zone ice, which appears laminated in the radar records, provides a reasonably strong reflection at its upper interface, presumably due to the sharp increase in debris content. Radar profiling to and along marginal exposures of basal ice shows that the basal-ice zone produces numerous short reflection segments and diffractions. In addition, the bottom of the basal zone can usually be identified by a concentration of such features overlying a quieter zone in the radar records (Arcone and others, 1995). This ice–substrate contact is not always visible and typically cannot be located exactly, but allows approximate determination of ice thickness in many places below the ice–sediment interface. A bedrock reflector is not present however (Arcone and others, 1995). When combined with the reflection characteristics, this indicates at least several meters of sediment between the sole of the glacier and bedrock. A single borehole drilled about 50 m down-glacier of the deepest part of the overdeepening in 1997 encountered over 10 m of subglacial sediment, confirming this interpretation.

Elevation-corrected GPR profiles were used to estimate the bed slope out of the overdeepening (Fig. 9). Because the ice–sediment interface is not well defined in most records, the top of the easily recognized basal-zone ice was used to estimate the slope of the bed. Depth on each GPR profile was defined using a dielectric constant of 3.2 for the clean, englacial ice and 3.8 for the basal ice (Arcone and others, 1995). The typical basal slope is about 0.25. Survey data show that the ice surface generally slopes down-glacier at a gradient of approximately −0.05. Thus, the ratio of the bed to surface slope is roughly −5 and meets the conditions required for supercooling within a subglacial drainage system. If all of an 8 m thick layer of basal ice grew in the overdeepening, then the bed slope is about 20% more gradual than the top of the basal zone, yielding a bed/surface slope ratio of −4 that would still allow supercooling.

GPR data also indicate that the basal-zone ice exists in areas peripheral to the ice-marginal overdeepening (Lawson and others, 1991; Arcone and others, 1995). Up-glacier of some of these areas, recent thinning of the glacier has accentuated crevasse patterns and ice-surface topography similar to those of the ice-marginal overdeepening (Fig. 3), suggesting that basal-ice accretion is occurring in multiple overdeepenings beneath the terminal lobe of the glacier. Crevasse patterns and surface-slope data suggest that additional overdeepenings probably occur several or more kilometers further up-glacier, a situation which is not unexpected (Hooke, 1991).

Many of the radar events near the bottom of the apparent basal-zone ice are interpreted as air- or water-filled spaces, based upon the phase polarity of the reflected waveforms (Arcone and others, 1995). Profiles obtained along the

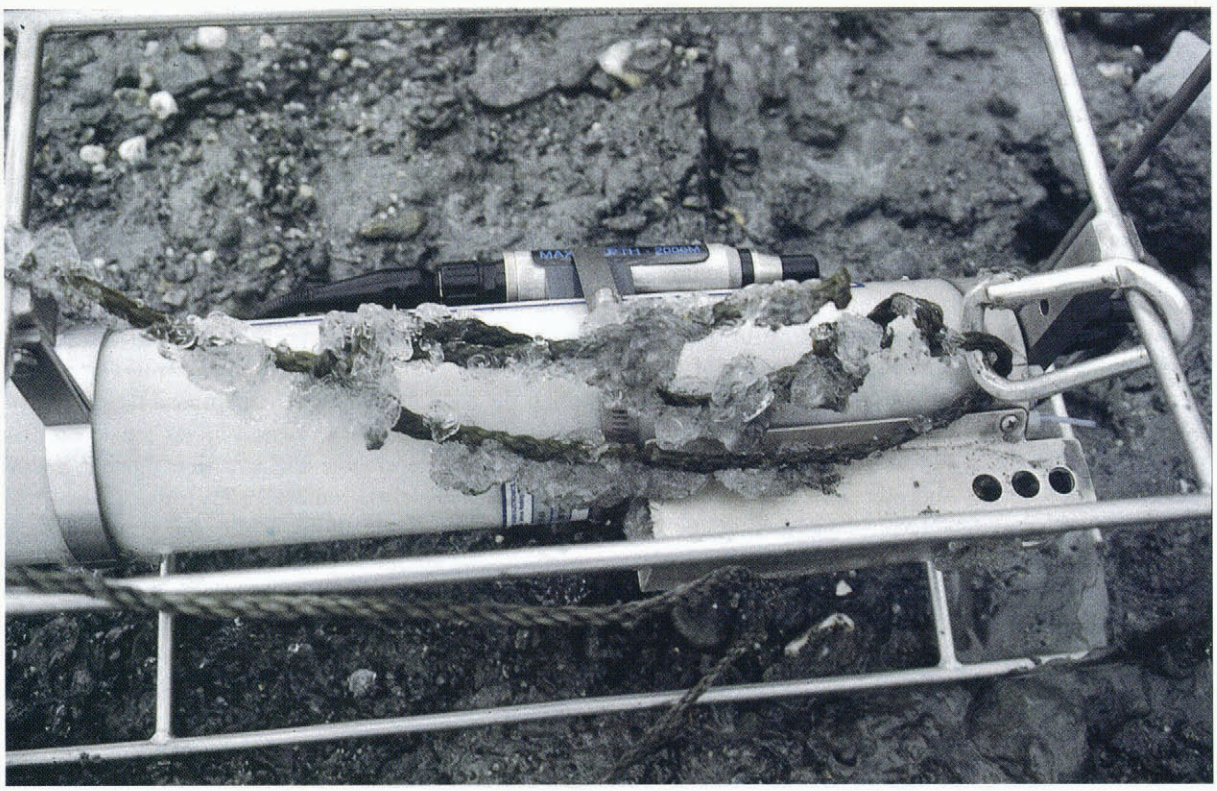

Fig. 6. Ice crystals, some in the form of rosettes, that grew on the rope and metal cage of an instrument (CTD unit) suspended in an active vent.

https://doi.org/10.3189/S0022143000002069 Published online by Cambridge University Press

Fig. 7. Large ice terrace, with about 1.5 m of height exposed, over which water from a central fountain flows into an outlet stream. The full thickness of the terrace was over 2.5 m and covered an area of several tens of square meters around the fountain. Vegetated slopes in the background cover stagnant glacier ice.

edge of the glacier (e.g. Arcone and others, 1995, fig. 8) above the vents show that such reflections correlate directly with known locations of conduits. Additional profiles along transects paralleling the ice margin show a progressive increase in the number of these reflections with distance up-glacier into the overdeepening. We suggest that this represents an increase in the number of conduits and cavities, and thus the existence of a distributed drainage system (e.g. Walder, 1986; Walder and Fowler, 1994). This is consistent with the results discussed by Hooke (1998, p. 150), which indicate that a highly branched, distributed network of water conduits is typical across overdeepenings.

Our inference of a distributed subglacial hydraulic system rising from the overdeepening is supported by dye-tracer experiments performed in August 1993. An example of these data (Fig. 10) shows concentrations of rhodamine WT dye in water sampled from a vent every 4 min following its introduction as a 20% solution in a moulin approximately 580 m (straight-line distance) up-glacier of that vent. The multiple peaks suggest multiple, interconnected channels of various lengths, and/or temporary storage within cavities (e.g. Collins, 1978; Hooke and others, 1988; Seaberg and others, 1988; Willis and others, 1990). The length of time over which dye was detected also suggests significant dispersion, with the dyed water being diluted by other water intercepted during flow.

The average flow velocity from dye introduction to the peak return concentration is only 0.04 m s^{-1}, similar to velocities observed by Hooke and Pohjola (1994) for flow across an overdeepening of Storglaciären, Sweden. Calculations following Seaberg and others (1988), using their preferred channel roughness and assuming that the head gradient for water flow is that given by ice pressure and bed elevation, indicate that water-flow paths have hydraulic radii of roughly 14 mm. Discharge at Matanuska Glacier occurs through multiple vents more than an order of magnitude larger than this, so the flow must be highly divided, distributed or constricted along much of its path. The high volume of suspended solids in the emerging flow indicates a significant subglacial contribution of sediment, and the August testing is at a time when channel development should be near its maximum, so we infer that much water flow is routed through a distributed basal system across the overdeepening during most of the melt season.

EVIDENCE FOR SUBGLACIAL ACCRETION

Characteristics of basal ice and debris provide evidence for the fairly recent (post-nuclear testing) accretion of ice to the sole of the glacier and entrainment of sediment during its growth. The physical properties of the glacier's basal zone were first described in detail by Lawson (1979a, b), who classified the zone into an upper "dispersed facies" and a lower "stratified facies". The dispersed-facies ice differs from the white, nearly debris-free englacial ice above it in having a slightly higher debris content (~5%) and smaller grain-size (Lawson and Kulla, 1978), while the stratified facies has physical and chemical attributes that are unique from both the dispersed facies and the englacial ice (Lawson and Kulla, 1978).

The stratified facies, the origin of which this paper addresses, typically ranges in thickness from 3 to 6 m in exposures, although sections of 8–10 m are not uncommon. The stratified facies is extremely complex and variable. Generally, it consists of alternating, subhorizontal lenses of debris-rich, debris-poor and debris-free ice, most of which are 5–20 mm thick (Fig. 11). In three dimensions, the lenses

https://doi.org/10.3189/S0022143000002069 Published online by Cambridge University Press

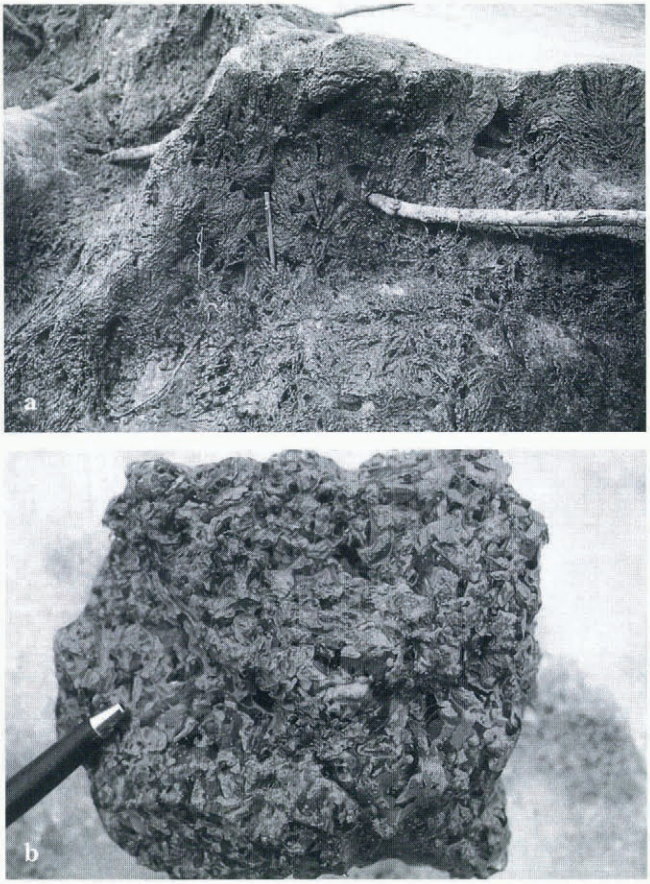

Fig. 8. Sediment in ice of vents and terraces. (a) Sediment-laden platy ice mass exposed at low flow within the large ice terrace shown in Figure 7. The open framework of the crystals creates innumerable interstitial cavities within which sediment is trapped as water seeps through the cavities. Additional ice grows epitaxially to close pore spaces. Large plates are evident surrounding the pen and the ice-engulfed willow branch. (b) Indurated, debris-rich ice formed within a vent cavity during summer 1993. Sediment is trapped between ice crystals about 5 mm across. Slight melting is beginning to concentrate sediment on the surface of the sample.

typically extend only 1–2 m along and into the ice face. The grain-sizes of debris in individual horizons range widely from clay to cobbles, but as a composite are pebbly-sandy silt. Intercalated with debris-rich laminae are lenses and layers of clear, bubble-free ice without debris or with widely separated aggregates that vary in composition from silt and fine sand to pebbly silt (diamictons). Sparse small-amplitude folds and disturbed foliation including minor faults suggest that only limited deformation of stratified ice has occurred. (Metamorphic foliation developed by large strains can exhibit small-amplitude disturbances; however, we consider it highly unlikely that the basal-ice foliation records large strain, based on the detailed appearance of the ice and on the high strain rates that such an explanation would imply, as described below.)

The mean debris concentration in individual layers is most commonly 15–60% by volume, but ranges from nearly zero to over 95%, similar to that of frazil and anchor ice. Vertically decreasing or increasing trends in debris concentration in a section are rare.

Recently completed co-isotopic analyses of ice and water sources from the Matanuska basin (Fig. 12), together with the earlier analyses of Lawson and Kulla (1978), provide further evidence for subglacial ice accretion. Our preliminary results (Lawson and others, 1996) indicate that:

(1) The englacial-zone ice is isotopically lighter than the stratified-facies ice (Figs 12a and 13).

(2) The isotopic composition of the stratified-facies ice cannot be developed by a closed-system fractionation of englacial meltwater in which a significant fraction of the englacial source is refrozen (Fig. 12a).

(3) The isotopic composition of stratified-facies ice is consistent with fractionation during partial freezing of subglacial water in an open system (Fig. 12b), one in which the remaining water is continuously removed and replenished by water of similar isotopic composition (O'Neil, 1968; Arnason, 1969; Souchez and Jouzel, 1984; Lehmann and Siegenthaler, 1991).

(4) Frazil and anchor ice are isotopically indistinguishable from stratified-facies ice (Fig. 12c).

(5) Clear-ice layers have nearly the same isotopic composition as debris-rich horizons in contact with them, supporting the notion that their source water was continuously being replaced by water of similar composition within an open system (Fig. 12d). Multiple samples from individual thick layers and lenses of clear ice, or of ice with suspended sediment, show no systematic differences in composition within individual layers.

The presence of bomb-produced tritium (^{3}H) in stratified-facies ice but not in overlying englacial ice (Fig. 13) demonstrates that meteoric water from the last 40–50 years is a significant component of the basal ice, and thus that much of the basal zone is relatively young (Larson and others, 1994; Strasser and others, 1996a, b). Sections from ice that passed through the ice-marginal overdeepening (Fig. 3; Strasser and others, 1996b) and from ice that traversed overdeepenings located farther up-glacier (Fig. 13) contain tritium. In addition, bomb tritium concentrations in precipitation (7–8 TU) and subglacial waters (5–8 TU) are similar to those of frazil and anchor ice growing in ice-marginal vents. Groundwater near the terminus in mid-winter has concentrations similar to precipitation (~5 TU). Of note is the fact that the lowermost ice of the stratified facies has tritium concentrations comparable to those of both modern frazil ice and subglacial waters (Strasser and others, 1996b). In addition, the profile of tritium with increasing depth in the stratified facies is quite similar to the profile of tritium in regional precipitation since the late 1950s (see Strasser and others, 1996b, fig. 7, p. 131).

We conclude from both the stable-isotopic and tritium analyses that the ice composing the stratified facies is derived from water in the subglacial drainage system and that the basal ice must have been accreted to the glacier's sole, with the net growth direction downward. These stable and radioisotopic data also provide much information on the relative contributions of recent precipitation, older groundwater, and englacial-ice melting to this subglacial discharge, but the large quantity and complexity of these data require detailed discussions that are beyond the scope of this paper.

In addition to the isotopic evidence, many physical characteristics of the stratified facies support net accretion within, or in association with, the subglacial drainage system. They include:

https://doi.org/10.3189/S0022143000002069 Published online by Cambridge University Press

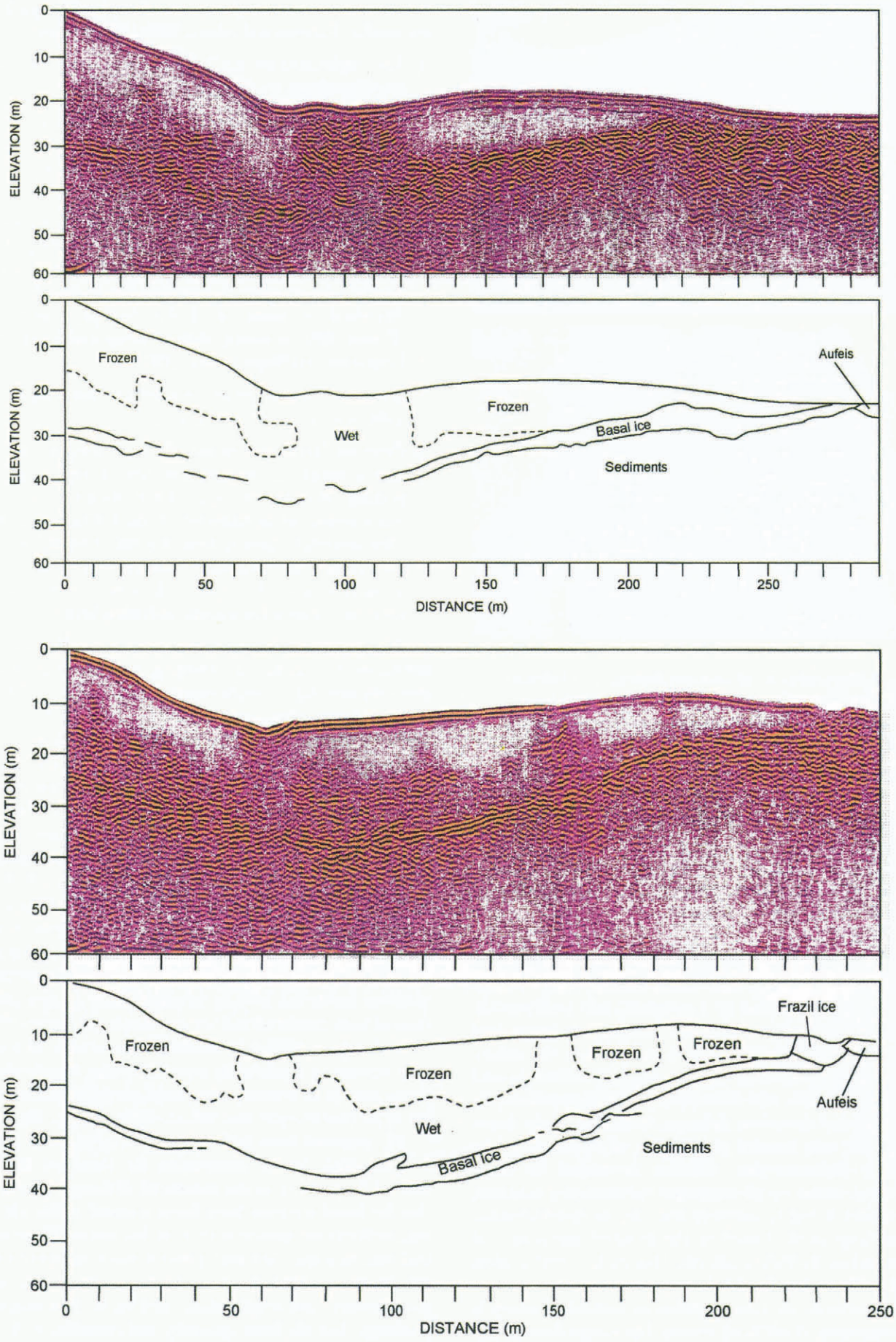

Fig. 9. Radar profiles and interpretations for two transects aligned approximately parallel to ice flow (left to right) through the overdeepening. Positive phase reflection is gold; negative phase is black. Three bands define a reflection. A regime of coherent reflections delineates the top of the basal zone, with a series of reflections and diffractions emanating from the basal ice, conduits and subglacial sediments beneath it. Surface slopes are locally up-glacier in low areas where radar was easy to drag across the surface, but average down-glacier in the region.

https://doi.org/10.3189/S0022143000002069 Published online by Cambridge University Press

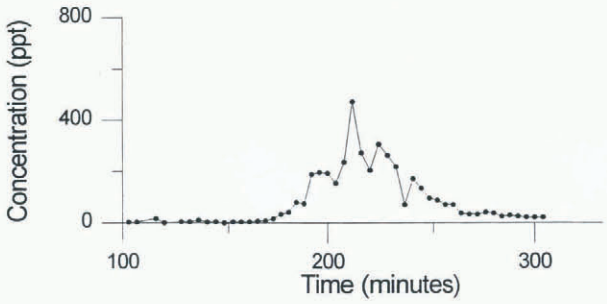

Fig. 10. Rhodamine dye concentrations in water samples from an ice-marginal vent; dye was released on 19 August in a moulin 580 m up-glacier of the terminus at time t = 0 min. Dye concentrations were measured on 21 August after suspended sediment settled out of each sample.

(1) Debris dispersal varies laterally and vertically in a section, with rapid changes in texture, sorting and ice volume (Fig. 14). Ice lenses and layers are clear, bubble-free and fine-grained (Lawson, 1979b). A few lenses are clast-supported, as would be expected for material incorporated by regelation into the bed with little subsequent modification (Iverson, 1993); however, most ice contains non-clast-supported debris in which silt is often the major component of individual strata, with a great similarity to terrace and other anchor ice, but not to regelation-entrained ice.

Fig. 11. Upper 3.5 m of stratified facies of the basal-zone ice exhibiting discontinuous layers and lenses of debris-laden and clear, bubble-free ice. Overall texture of the debris within the ice is a pebbly-sandy silt. Note that larger clasts are few and dispersed throughout the section. Ice flows approximately left to right.

(2) Discontinuous lenses of ice-rich sediment and sediment-rich ice occasionally exhibit a channel form (Fig. 15) that is wider than it is high (commonly <0.1 m high; <1.0 m wide), similar to englacial and subglacial conduits at the ice margin, and as would be expected in subglacial channels or canals (Hooke, 1991; Walder and Fowler, 1994). Debris within these lenses is typically rounded, well sorted and sometimes stratified, or exhibits vertical gradations in size. These properties suggest fluvial deposition in conduits, and perhaps en masse entrainment. Our ability to recognize such channel-form deposits, combined with their rarity and the more common occurrence of features with even more extreme aspect ratios, is consistent with occurrence of channels but dominance of accretion from more-distributed waterflow paths.

(3) Debris-rich lenses and layers may contain well-sorted sands, gravels, clay and silt, as well as aggregates of mixed grain-sizes (diamictons) (Fig. 16a), suggesting both fluvial and bed-material origins. Debris-rich strata containing coarser debris often alternate with ice-rich strata of finer-grained debris (Fig. 16b).

(4) Pebble- to boulder-sized clasts, which are most often widely separated throughout the section (Fig. 11), are only rarely striated or faceted and are often fluvially shaped (Lawson, 1979a, b). These properties suggest only limited or no interaction between the glacier sole and bed prior to or during the incorporation of clasts into basal ice.

(5) Sedimentary structures, such as ripple cross-laminations, graded strata and parallel bedding, are relatively rare but do occur. Sedimentary structures in lenses and discontinuous layers indicate that some sediment is incorporated en masse, that internal shearing or other deformation of the ice containing this sediment has been limited, and that basal debris was in part derived from fluvial sediments. Some of these features possibly record processes in englacial channels, but their rarity, and the rarity of any channel-form features, indicate that any contribution of englacial channels to formation of the debris-rich basal ice is minor.

(6) Small (millimeter-size), irregular to star-shaped aggregates of sandy silt to silt (identical texturally to the Matanuska River suspended-sediment load) are, in some instances, uniformly suspended within clear ice (Fig. 17a), forming discontinuous layers or lenses ten to hundreds of millimeters thick. These aggregates usually lie within voids at three- and four-grain intersections and between grain boundaries. These suspended-subfacies horizons have debris dispersal, content and form nearly identical to indurated, sediment-rich frazil deposits that we have observed growing in vent mouths from supercooled water (Fig. 17b).

We have been unable to use any of the current hypotheses on the origin of basal zones and the entrainment of sediment by glaciers (reviewed by Alley and others, 1997) to account adequately for the combined physical and chemical properties of the stratified facies at Matanuska Glacier. These hypotheses generally rely on regelation, the localized pressure-melting and refreezing of ice (Kamb and LaChapelle, 1964; Weertman, 1964; Robin, 1976; Iverson, 1993), or

https://doi.org/10.3189/S0022143000002069 Published online by Cambridge University Press

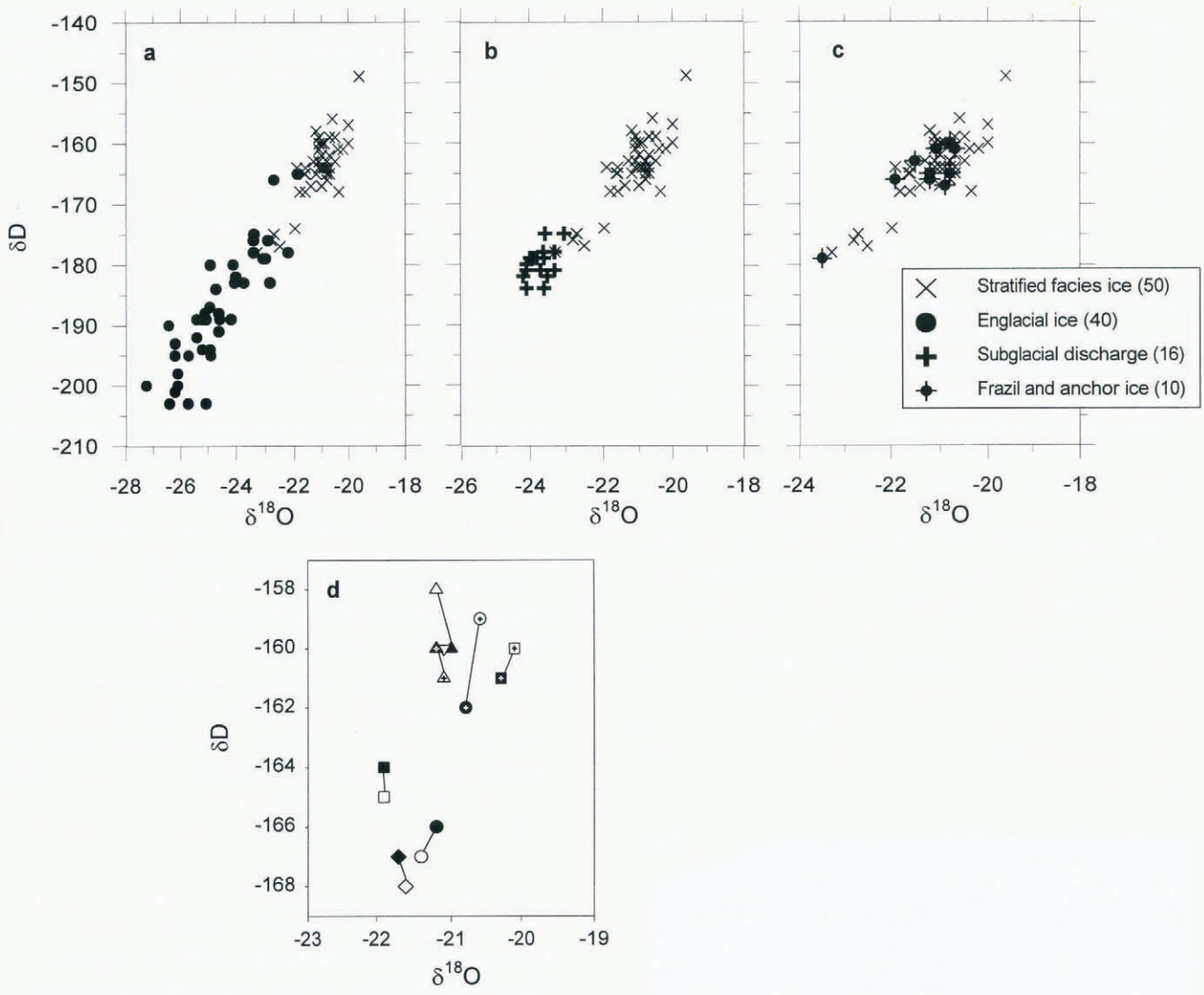

Fig. 12. Co-isotopic composition of water and ice in Matanuska Glacier's terminus region. (a) Isotopic composition of englacial-zone ice compared to that of stratified-facies ice. (b) Isotopic composition of the stratified-facies ice compared to the waters discharging from subglacial conduits at the glacier's margin. (c) Isotopic composition of stratified-facies ice compared to that of recently formed frazil and anchor ice at Matanuska Glacier's margin. (d) Isotopic composition of pairs of a clear, debris-free ice layer (solid symbol) and a debris-rich layer (open symbol) (one pair is identical and plots as a single point). The number of samples analyzed is indicated in parentheses in the legend.

thermal conditions at the bed that result in the bulk freeze-on of sediment and water (e.g. Weertman, 1961; Boulton, 1972). However, we do not discount the existence of other mechanisms in entraining sediment and creating basal ice; in fact, we assume that regelation and other mechanisms have contributed to development of Matanuska Glacier's stratified facies. We consider the basal-zone ice to be the product of multiple processes that can vary in importance.

We conclude, however, that the assemblage of debris and ice properties at Matanuska Glacier shows the primary origin of the stratified facies to be the growth of ice from subglacially supercooled water. In our companion paper (Alley and others, 1998), we demonstrate theoretically that this freeze-on mechanism can accrete meters-thick sections of debris-laden ice over tens of years or less, as observed.

SIGNIFICANCE

Glaciohydraulic supercooling can rapidly entrain sediment in growing basal ice, producing significant sediment flux within the glacier. Ice accretes in response to hydraulically regulated temperature and pressure changes; therefore, the supercooling mechanism is likely to be active beneath any glacier that flows through a sufficiently steep overdeepening and has periods of high water flux within a distributed subglacial drainage system. Overdeepenings are common beneath glaciers of all sizes, from cirque glaciers to continental ice sheets, so it is reasonable to expect that operation of this mechanism currently is not and has not been restricted to Matanuska Glacier. Frazil ice in subglacial discharges has recently been reported emerging from upwellings within the lake abutting the surging Bering Glacier in Alaska (Fleisher and others, 1996, 1997), and was observed at Aktineg Glacier on Bylot Island, Arctic Archipelago, by one of us (E.B.E.), both cases being consistent with this hypothesis. Röthlisberger and Lang (1987) have also described ice mounds growing around an apparent upwelling (artesian) discharge at Griesgletscher in Switzerland.

Supercooling in overdeepened basins may be important to the moraine-building process, a process that can be self-sustaining along a stable margin. The continuous entrain-

https://doi.org/10.3189/S0022143000002069 Published online by Cambridge University Press

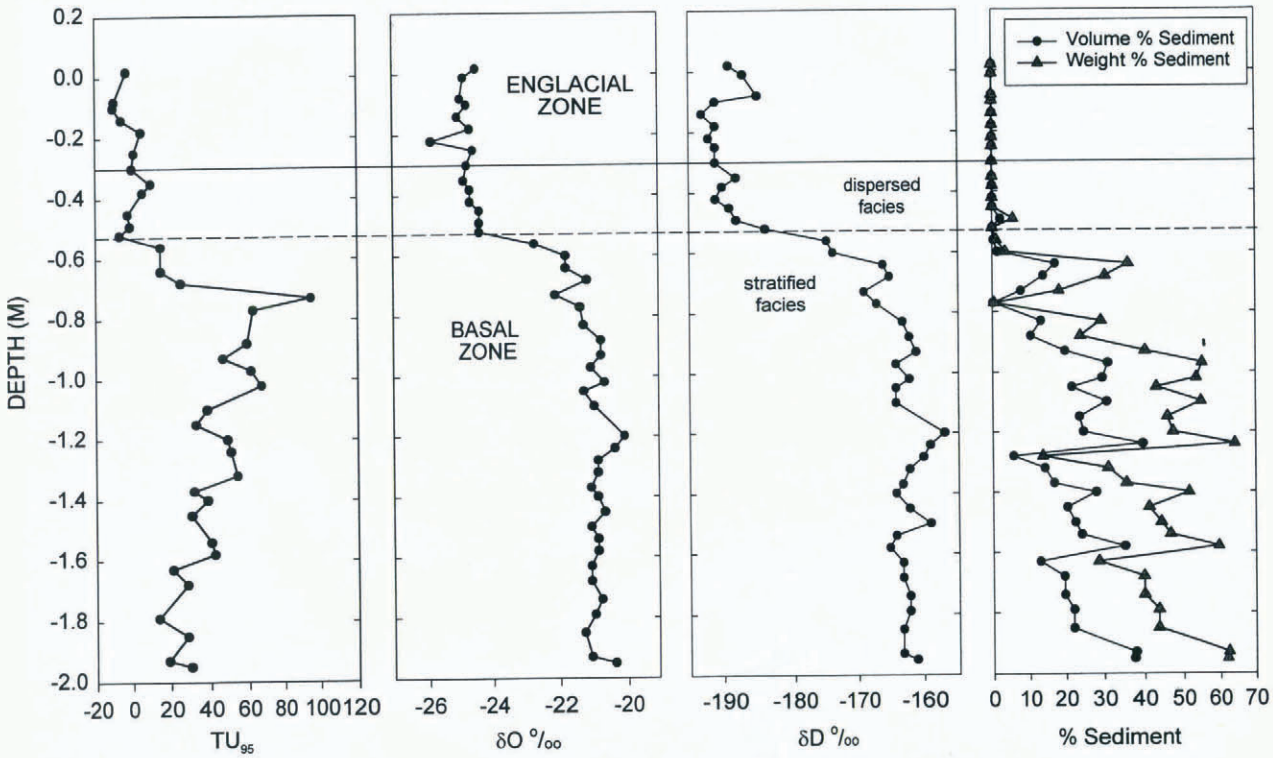

Fig. 13. Vertical profiles, from left to right, of the tritium (±10 TU) content, oxygen (±0.3‰) and hydrogen (±5.0‰) isotope ratios and debris volume from a section which lies just south of the ice-marginal overdeepening but west of a second, up-glacier overdeepening (Fig. 3). The isotopic composition changes at the contact of the dispersed and stratified facies; the apparent gradational nature of this change is under investigation. Samples represented by each dot are from cores 50 mm in diameter and 100 mm in length. Depth is relative to an arbitrary datum.

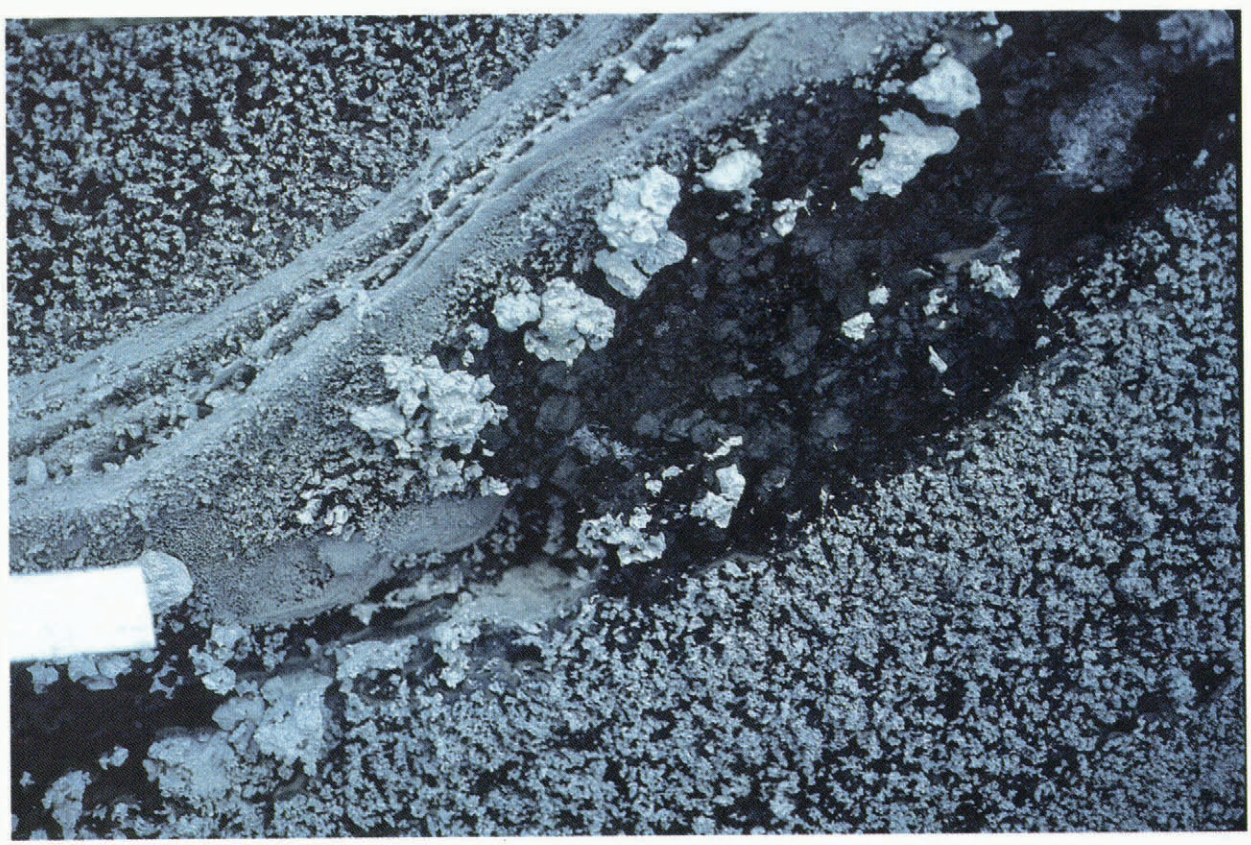

Fig. 14. Detailed view showing highly variable modes of debris dispersal. Diamict aggregates at photo center occur suspended in clear, bubble-free ice. Several thin (3–10 mm) debris-rich layers of silty sand to sandy silt alternating with 10 mm ice-rich layers lie below the bubble-free ice. The upper one-third of the photograph shows several diffusely laminated horizons of silt-rich aggregates (referred to as suspended subfacies layers), while a massive suspended subfacies horizon occurs in the lower right. Ice flow is approximately left to right. Length of scale shown is about 40 mm.

https://doi.org/10.3189/S0022143000002069 Published online by Cambridge University Press

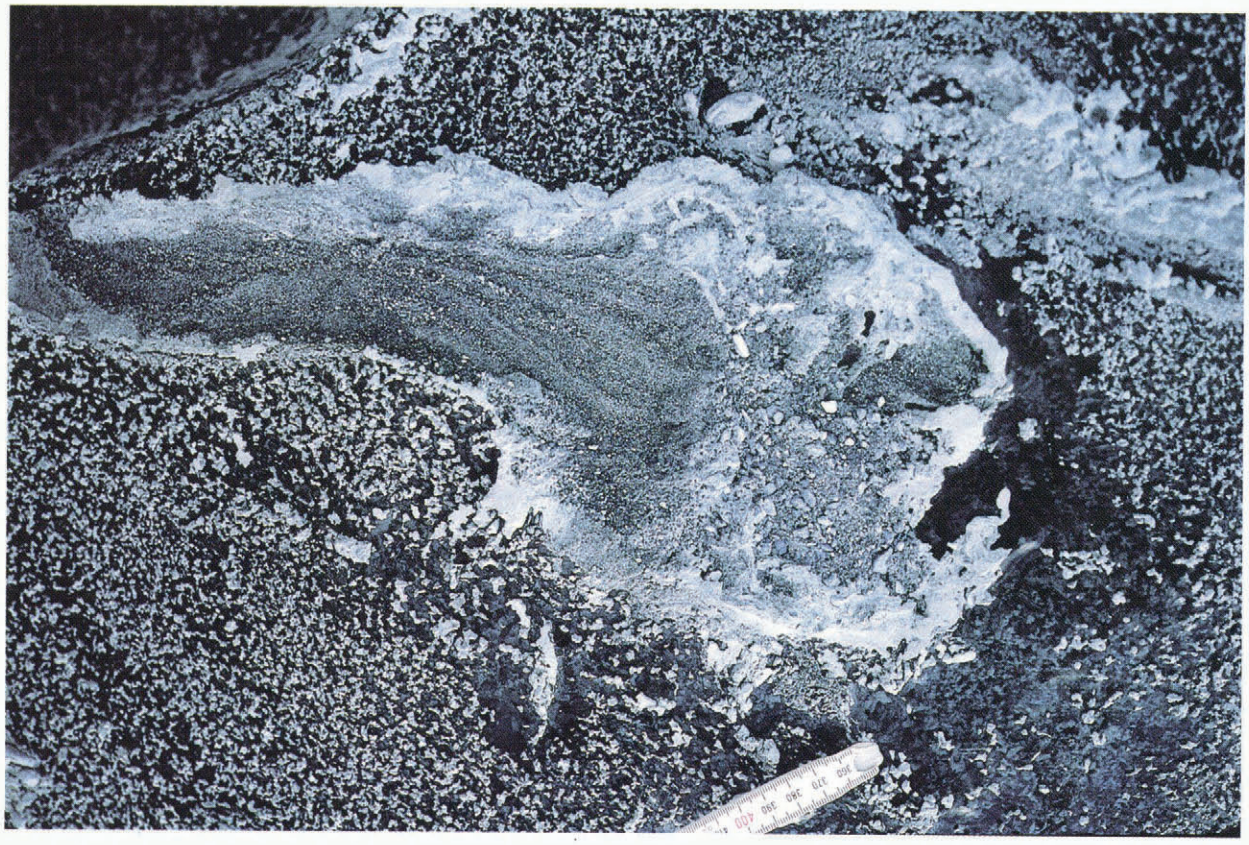

Fig. 15. Planar view of cavity-like deposit exposed on the inclined bottom of an overthrust section of the glacier margin. Ice flow was from left to right above the photographer.

ment of sediment deepens the basin. The continuous flux of large quantities of sediment up the backslope of the end moraine and deposition along the ice margin increases the height of the ridge, impeding flow and lengthening the bed slope. Overthrusting during winter, and burial of basal ice, lead to reworking and resedimentation of basally derived materials (Lawson, 1979b). Some of these materials are lost to streams, but the remainder form moraines. In addition, because sediments in the subglacial fluvial system are normally removed from the glacier's immediate environs, ice accretion by the supercooling mechanism is a way by which glaciofluvial sediment can be retained and become a part of the glacier's basal load. Following release from buried or exposed ice, it becomes a component of the melt-out till or resedimented diamictons that make up end moraines (Lawson, 1979b, 1981; Lawson and others, 1996). Thus, the supercooling mechanism may have contributed to the morainal deposits down-glacier of the Great Lakes and similar prominent overdeepenings along the Laurentian ice-sheet margin.

In tidewater situations, the submarine moraine (Powell, 1981) along stable or advancing ice margins may provide the necessary bed slope for supercooling. This could account for the apparent freeze-on of 0.1–1 m thick strata that have been identified in basal ice at some tidewater margins (e.g. Hunter and others, 1996). If so, sediment entrainment and basal-ice formation will move subglacial material to the ice face, where submarine melting may release it or calving may release icebergs bearing it. We speculate that if sufficient subglacial water was available, this process may have contributed to debris entrainment in ice passing through the Hudson Strait overdeepening to create Heinrich events (Heinrich, 1988; Alley and MacAyeal, 1994; Dowdeswell and others, 1995).

CONCLUSIONS

Water flowing from an overdeepening beneath Matanuska Glacier is supercooled when it emerges from ice-marginal vents, and grows ice around the vents even when air temperatures are well above freezing. The water contains suspended frazil ice, indicating that supercooling extends some unknown distance up-glacier. The stratified, debris-rich basal ice of the glacier is isotopically very similar to ice growing around the vents, but isotopically distinct from the bulk of the glacier, both in terms of stable isotopes of water and in terms of bomb-produced tritium content. Physical characteristics of the basal ice and its debris are in some cases nearly identical to those of the vent ice, and are all explainable by growth of ice from supercooled water with associated trapping of sediment from that water.

Water flowing from overdeepenings can become supercooled if the pressure drop along flow causes the pressure-melting point to rise more rapidly than the water is heated by the viscous dissipation of the flowing water. The criterion for supercooling (adverse bed slope >1.2–1.7 times the magnitude of the surface slope) is met for the overdeepening near the terminus of Matanuska Glacier, which has an adverse bed slope approximately 5 times the magnitude of the surface slope. Based on theory and observations on other glaciers (e.g. Röthlisberger, 1972; Hooke, 1989), large channels rising from such an overdeepening are expected to freeze closed, diverting water flow into a distributed englacial or basal drainage system (e.g. Weertman, 1972; Walder and Fowler, 1994). Dye-tracing and other observations at Matanuska Glacier demonstrate that a distributed and at least partially basal drainage system does supply the supercooled water to the ice-marginal vents.

We thus conclude that widespread basal ice growth is

https://doi.org/10.3189/S0022143000002069 Published online by Cambridge University Press

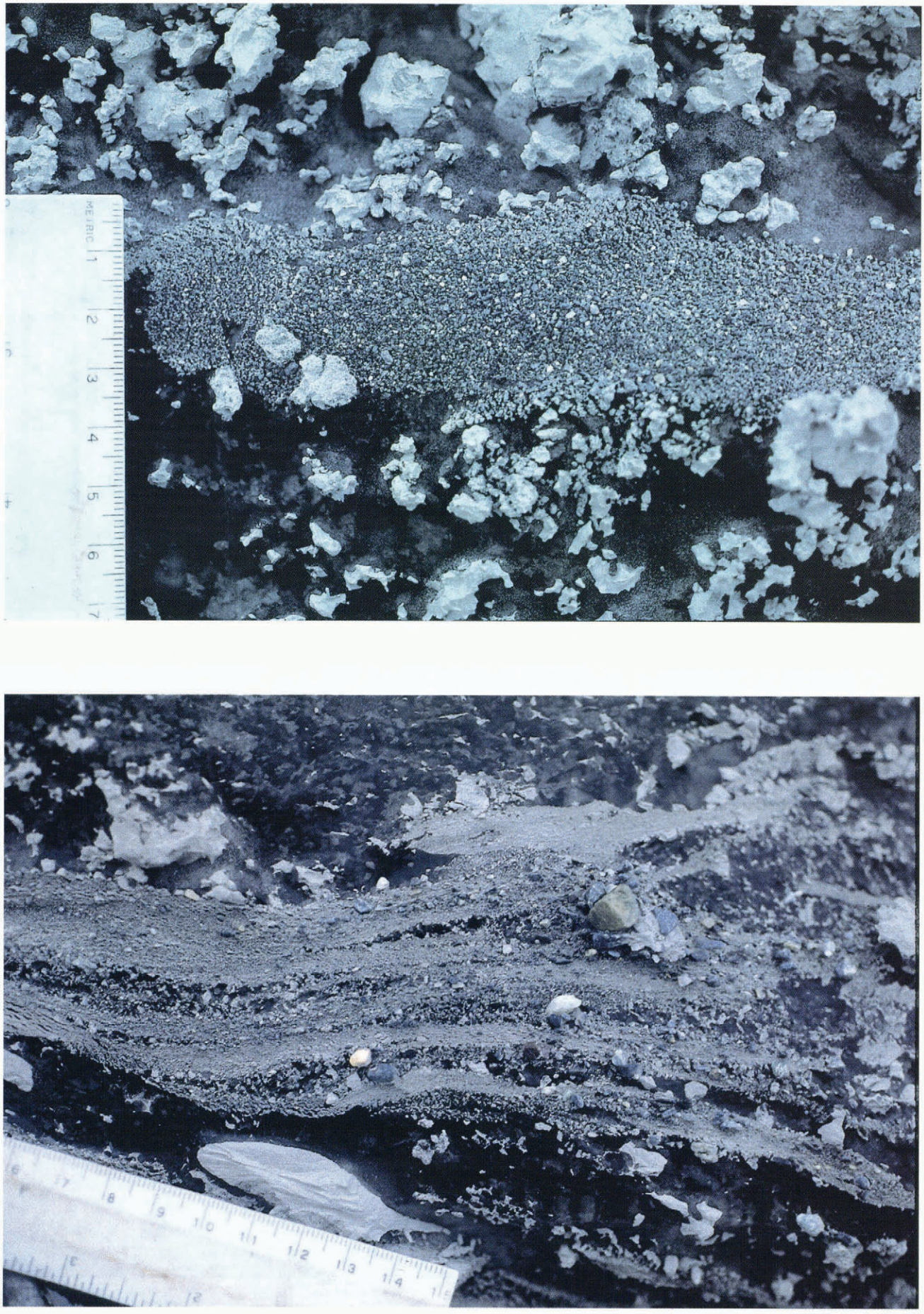

Fig. 16. (a) Well-sorted coarse sand lens (center) and clear ice horizons (top and bottom) containing suspended aggregates of silt. (b) Subhorizontally stratified basal ice containing silt, pebbly coarse sand, silty sand and sand layers, in which only small clear ice lenses are present. Debris appears distinctly fluvial in origin. Scale is about 80 mm long. View is approximately perpendicular to the ice flow.

https://doi.org/10.3189/S0022143000002069 Published online by Cambridge University Press

a

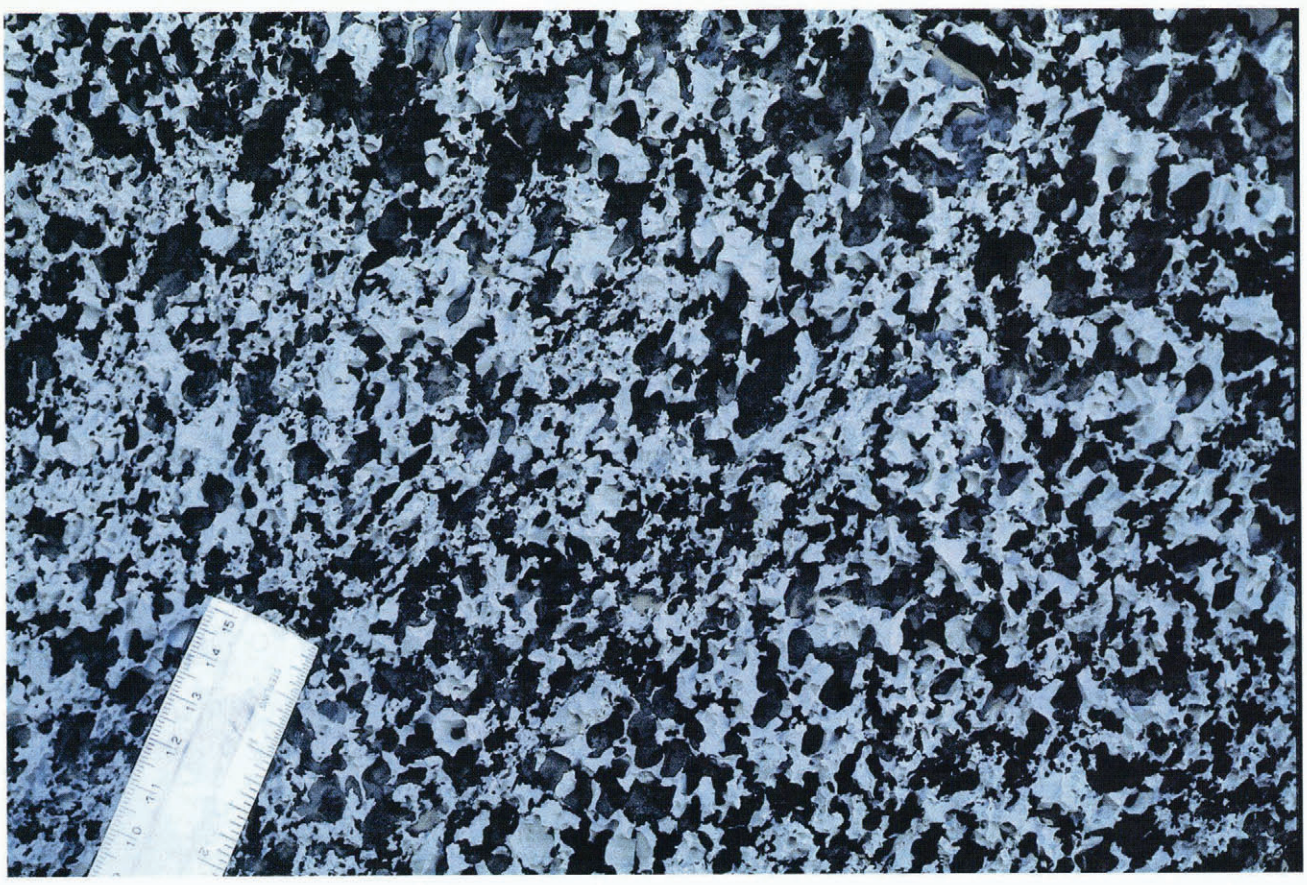

b

Fig. 17. Physical similarity of sediment-laden frazil ice and the suspended subfacies of the stratified basal ice. (a) Suspended subfacies ice exhibiting irregular and star-shaped aggregates of sandy silt within clear, bubble-free ice. Note the relatively uniform dispersal of these aggregates. Smallest-scale gradations are millimeters. Surface relief of the debris results from sublimation of the surrounding ice. (b) Recently formed frazil-ice mass containing irregular and star-shaped aggregates of sandy silt in bubble-free clear ice. View is about 200 mm across.

https://doi.org/10.3189/S0022143000002069 Published online by Cambridge University Press

occurring from supercooled water rising along the bed of Matanuska Glacier. Growth rates of a few meters of ice in a few decades are documented by the presence of bomb tritium in sections lacking evidence of significant tectonic thickening. Typical sediment concentrations are tens of per cent by volume, so this mechanism entrains a lot of sediment that can contribute to moraine formation and other processes.

Ice growth around vents (Röthlisberger and Lang, 1987) and in subglacial discharges (Fleisher and others, 1997) has been observed elsewhere. Stratified basal ice occurs down-glacier from each overdeepening identified thus far in Matanuska Glacier's terminus region. Overdeepenings are also quite common beneath glaciers (Hooke, 1991), so it is likely that this mechanism functions beneath other glaciers and contributes to their sediment fluxes and deposits. The occurrence of prominent overdeepenings up-glacier from interesting features, including the Hudson Strait overdeepening through which Heinrich-event sediment apparently passed, and the Lake Michigan and Lake Superior overdeepenings through which the tills of Illinois and Wisconsin, respectively, passed, raises the possibility that hydraulic supercooling contributed to sediment flux in these and similar situations.

ACKNOWLEDGEMENTS

This research was supported by a grant to E. B. Evenson and D. E. Lawson from NSF (OPP 9223007) and by CRREL in the Civil Works Cold Regions Water Resources Program (CWIS32689, Predicting runoff and sediment yield from partly glacierized basins). J. C. Strasser's participation was funded in part by grants from GSA (4810-91 and 5055-92) and Sigma Xi. R. B. Alley thanks NSF OPP, NASA-EOS and the D. and L. Packard Foundation for funding. We thank N. Iverson and M. Sharp for insightful reviews, G. Ashton for helpful discussions on ice-growth mechanisms in supercooled water, J. Gosse for field assistance and discussions, E. Brodsky for conducting the dye-tracer experiments, and C. Farnsworth for assistance in preparation of the manuscript. A special thanks to W. and K. Stevenson for their camaraderie and enthusiastic support of our field operations.

REFERENCES

Alley, R. B. 1991. Deforming-bed origin for southern Laurentide till sheets? *J. Glaciol.*, **37**(125), 67–76.

Alley, R. B. and D. R. MacAyeal. 1994. Ice-rafted debris associated with binge/purge oscillations of the Laurentide ice sheet. *Paleoceanography*, **9**(4), 503–511.

Alley, R. B., K. M. Cuffey, E. B. Evenson, J. C. Strasser, D. E. Lawson and G. J. Larson. 1997. How glaciers entrain and transport sediment at their beds: physical constraints. *Quat. Sci. Rev.*, **16**, 1017–1038.

Alley, R. B., D. E. Lawson, E. B. Evenson, J. C. Strasser and G. J. Larson. 1998. Glaciohydraulic supercooling: a freeze-on mechanism to create stratified, debris-rich basal ice: II. Theory. *J. Glaciol.*, **44**(148), 563–569.

Arcone, S. A., D. E. Lawson and A. J. Delaney. 1995. Short-pulse radar wavelet recovery and resolution of dielectric contrasts within englacial and basal ice of Matanuska Glacier, Alaska, U.S.A. *J. Glaciol.*, **41**(137), 68–86.

Arnason, B. 1969. Equilibrium constant for the fractionation of deuterium between ice and water. *J. Phys. Chem.*, **73**(10), 3491–3494.

Ashton, G. D. 1983. Frazil ice. *In* Meyer, R. E., *ed. Theory of dispersed multiphase flow.* New York, Academic Press Inc., 271–289.

Ashton, G. D. 1986. *River and lake ice engineering.* Littleton, CO, Water Resources Publications.

Boulton, G. S. 1970. On the deposition of subglacial and melt-out tills at the margins of certain Svalbard glaciers. *J. Glaciol.*, **9**(56), 231–245.

Boulton, G. S. 1972. The role of thermal régime in glacial sedimentation. *In* Price, R. J. and D. E. Sugden, *comps. Polar geomorphology.* London, Institute of British Geographers, 1–19.

Collins, D. N. 1978. Hydrology of an Alpine glacier as indicated by the chemical composition of meltwater. *Z. Gletscherkd. Glazialgeol.*, **13**(1–2), 1977, 219–238.

Daly, S. F. 1994. Frazil ice dynamics. *CRREL Spec. Rep.* 94-23, 19–24.

Dowdeswell, J. A., M. A. Maslin, J. T. Andrews and I. N. McCave. 1995. Iceberg production, debris rafting, and the extent and thickness of Heinrich layers (H-1, H-2) in North Atlantic sediments. *Geology*, **23**(4), 302–304.

Echelmeyer, K. and W. Zhongxiang. 1987. Direct observation of basal sliding and deformation of basal drift at sub-freezing temperatures. *J. Glaciol.*, **33**(113), 83–98.

Fleisher, P. J., E. H. Muller, D. H. Cadwell, C. L. Rosenfeld and P. K. Bailey. 1996. Subglacial conduit system endures repeated surges, Bering Glacier, Alaska. *Geol. Soc. Am. Abstr. Programs*, **28**(3), 54.

Fleisher, P. J., D. H. Cadwell, E. H. Muller and B. B. Tormey. 1997. Abundant renewal of frazil ice, Tsivat Lake, Bering Glacier, AK. [Abstract.] *EOS*, **78**(46), Fall Meeting Supplement, F251.

Forest, T. 1994. Physics of frazil ice. *CRREL Spec. Rep.* 94-23, 1–4.

Gow, A. J., S. Epstein and W. Sheehy. 1979. On the origin of stratified debris in ice cores from the bottom of the Antarctic ice sheet. *J. Glaciol.*, **23**(89), 185–192.

Heinrich, H. 1988. Origin and consequences of cyclic ice rafting in the northeast Atlantic Ocean during the past 130,000 years. *Quat. Res.*, **29**(2), 142–152.

Herron, S. and C. C. Langway, Jr. 1979. The debris-laden ice at the bottom of the Greenland ice sheet. *J. Glaciol.*, **23**(89), 193–207.

Hooke, R. LeB. 1989. Englacial and subglacial hydrology: a qualitative review. *Arct. Alp. Res.*, **21**(3), 221–233.

Hooke, R. LeB. 1991. Positive feedbacks associated with erosion of glacial cirques and overdeepenings. *Geol. Soc. Am. Bull.*, **103**(8), 1104–1108.

Hooke, R. LeB. 1998. *Principles of glacier mechanics.* Upper Saddle River, NJ, Prentice-Hall.

Hooke, R. LeB. and V. A. Pohjola. 1994. Hydrology of a segment of a glacier situated in an overdeepening, Storglaciären, Sweden. *J. Glaciol.*, **40**(134), 140–148.

Hooke, R. LeB., S. B. Miller and J. Kohler. 1988. Character of the englacial and subglacial drainage system in the upper part of the ablation area of Storglaciären, Sweden. *J. Glaciol.*, **34**(117), 228–231.

Hubbard, B. and M. Sharp. 1995. Basal ice facies and their formation in the western Alps. *Arct. Alp. Res.*, **27**(4), 301–310.

Hunter, L. E., R. D. Powell and D. E. Lawson. 1996. Flux of debris transported by ice at three Alaskan tidewater glaciers. *J. Glaciol.*, **42**(140), 123–135.

Iverson, N. R. 1993. Regelation of ice through debris at glacier beds: implications for sediment transport. *Geology*, **21**(6), 559–562.

Iverson, N. R. and D. J. Semmens. 1995. Intrusion of ice into porous media by regelation: a mechanism of sediment entrainment by glaciers. *J. Geophys. Res.*, **100**(B7), 10,219–10,230.

Kamb, B. and E. LaChapelle. 1964. Direct observation of the mechanism of glacier sliding over bedrock. *J. Glaciol.*, **5**(38), 159–172.

Larson, G. J., E. B. Strasser, E. B. Evenson and D. E. Lawson. 1994. Recent net freeze-on to the base of the Matanuska Glacier, as indicated by ^{3}H, $\delta^{18}O$, and δD. *Program with Abstracts, 19th Joint Annual Meeting, Geological Association of Canada and Mineralogical Association of Canada*, **19**, 61.

Lawson, D. E. 1979a. A comparison of the pebble orientations in ice and deposits of the Matanuska Glacier, Alaska. *J. Geol.*, **87**(6), 629–645.

Lawson, D. E. 1979b. Sedimentological analysis of the western terminus region of the Matanuska Glacier, Alaska. *CRREL Rep.* 79-9.

Lawson, D. E. 1981. Distinguishing characteristics of diamictons at the margin of the Matanuska Glacier, Alaska. *Ann. Glaciol.*, **2**, 78–84.

Lawson, D. E. 1988. Proxy data on subglacial conditions and processes. [Abstract.] *EOS*, **69**(44), 1210.

Lawson, D. E. 1993. Glaciohydrologic and glaciohydraulic effects on runoff and sediment yield in glacierized basins. *CRREL Monogr.* 93-02.

Lawson, D. E. and J. B. Kulla. 1978. An oxygen isotope investigation of the origin of the basal zone of the Matanuska Glacier, Alaska. *J. Geol.*, **86**(6), 673–685.

Lawson, D. E., S. A. Arcone and A. Delaney. 1991. Initial interpretation of VHF–UHF short-pulse radar profiles of the Matanuska Glacier, AK. [Abstract.] *EOS*, **72**(44), Supplement, 159.

Lawson, D. E., E. B. Evenson, J. C. Strasser, R. B. Alley and G. J. Larson. 1996. Subglacial supercooling, ice accretion, and sediment entrainment at the Matanuska Glacier, Alaska. [Abstract.] *Geol. Soc. Am. Abstr. Programs*, **28**(3), 75.

Lehmann, M. and U. Siegenthaler. 1991. Equilibrium oxygen- and hydrogen-isotope fractionation between ice and water. *J. Glaciol.*, **37**(125), 23–26.

Michel, B. 1978. *Ice mechanics.* Québec, Qué., Presses de L'Université Laval.

O'Neil, J. R. 1968. Hydrogen and oxygen isotope fractionation between ice

https://doi.org/10.3189/S0022143000002069 Published online by Cambridge University Press

and water. *J. Phys. Chem.*, **72**(10), 3683–3684.
Osterkamp, T. E. and J. P. Gosink. 1983. Frazil ice formation and ice cover development in interior Alaska streams. *Cold Reg. Sci. Technol.*, **8**(1), 43–56.
Powell, R. D. 1981. A model for sedimentation by tidewater glaciers. *Ann. Glaciol.*, **2**, 129–134.
Robin, G. de Q. 1976. Is the basal ice of a temperate glacier at the pressure melting point? *J. Glaciol.*, **16**(74), 183–196.
Röthlisberger, H. 1972. Water pressure in intra- and subglacial channels. *J. Glaciol.*, **11**(62), 177–203.
Röthlisberger, H. and H. Lang. 1987. Glacial hydrology. *In* Gurnell, A. M. and M. J. Clark, *eds. Glacio-fluvial sediment transfer: an alpine perspective.* Chichester, etc., John Wiley and Sons, 207–284.
Seaberg, S. Z., J. Z. Seaberg, R. LeB. Hooke and D. W. Wiberg. 1988. Character of the englacial and subglacial drainage system in the lower part of the ablation area of Storglaciären, Sweden, as revealed by dye-trace studies. *J. Glaciol.*, **34**(117), 217–227.
Sharp, M., J. Jouzel, B. Hubbard and W. Lawson. 1994. The character, structure and origin of the basal ice layer of a surge-type glacier. *J. Glaciol.*, **40**(135), 327–340.
Souchez, R. A. and J. Jouzel. 1984. On the isotopic composition in δD and δ^{18}O of water and ice during freezing. *J. Glaciol.*, **30**(106), 369–372.
Strasser, J. C., D. E. Lawson, E. B. Evenson and G. J. Larson. 1994. Crystallographic and mesoscale analyses of basal zone ice from the terminus of the Matanuska Glacier, Alaska: evidence for basal freeze-on in an open hydrologic system. [Abstract.] *Geol. Soc. Am. Abstr. Programs*, **26**(7), A177.
Strasser, J. C., E. B. Evenson, D. E. Lawson, G. I. Larson and R. B. Alley. 1996a. Freeze-on of tritium-enriched basal ice, Matanuska Glacier, Alaska. [Abstract.] *Geol. Soc. Am. Abstr. Programs*, **28**, 102.
Strasser, J. C., D. E. Lawson, G. J. Larson, E. B. Evenson and R. B. Alley. 1996b. Preliminary results of tritium analyses in basal ice, Matanuska Glacier, Alaska, U.S.A.: evidence for subglacial ice accretion. *Ann. Glaciol.*, **22**, 126–133.
Sugden, D. E. *and 6 others*. 1987a. Evidence for two zones of debris entrainment beneath the Greenland ice sheet. *Nature*, **328**(6127), 238–241.
Sugden, D. E., C. M. Clapperton, J. C. Gemmell and P. G. Knight. 1987b. Stable isotopes and debris in basal glacier ice, South Georgia, Southern Ocean. *J. Glaciol.*, **33**(115), 324–329.
Walder, J. S. 1986. Hydraulics of subglacial cavities. *J. Glaciol.*, **32**(112), 439–445.
Walder, J. S. and A. Fowler. 1994. Channelized subglacial drainage over a deformable bed. *J. Glaciol.*, **40**(134), 3–15.
Weertman, J. 1961. Mechanism for the formation of inner moraines found near the edge of cold ice caps and ice sheets. *J. Glaciol.*, **3**(30), 965–978.
Weertman, J. 1964. The theory of glacier sliding. *J. Glaciol.*, **5**(39), 287–303.
Weertman, J. 1972. General theory of water flow at the base of a glacier or ice sheet. *Rev. Geophys. Space Phys.*, **10**(1), 287–333.
Williams, J. R. and O. J. Ferrians, Jr. 1961. Late Wisconsin and recent history of the Matanuska Glacier, Alaska. *Arctic*, **14**(2), 83–90.
Willis, I. C., M. J. Sharp and K. S. Richards. 1990. Configuration of the drainage system of Midtdalsbreen, Norway, as indicated by dye-tracing experiments. *J. Glaciol.*, **36**(122), 89–101.

MS received 20 October 1996 and accepted in revised form 5 May 1998

https://doi.org/10.3189/S0022143000002069 Published online by Cambridge University Press